ISIMA Report on Collision Dynamics in Planet Formation

N. Wang

School of Astronomy & Space Sciences, Nanjing University

sanlia@126.com

S. Liu

Department of Earth & Planetary Sciences, UCSC

shangfei.liu@gmail.com

and

D. Valencia

Astrophysics Department, University of Toronto

dvalencia@utsc.utoronto.ca

Received _____; accepted _____

Work done in ISIMA 2014

ABSTRACT

The final stage of terrestrial planet formation in the solar system involves collisions between dozens of lunar-to-Mars-sized planetary embryos and the leftover planetesimals. Early N-body simulations have treated a collision as a perfect merger. Until recently, the importance of fragmentation and hit-and-run collisions has been taken into account.

Based on Leinhardt and Stewart's work (Leinhardt & Stewart 2012), we built a realistic collision model including four major regimes of merging, disruption, super-catastrophic disruption and hit-and-run, which were defined in their work. And we modified the REBOUND code (Rein & Liu 2010) to deal with different collisions and to track every body's collision history.

The future work is to continue the investigation of the effects of realistic collision model, by comparing the results of the simulations with fragmentation and those with merging only. In particular, the chemical composition of final products is of prime interest.

Subject headings: terrestrial planet, formation, collision, fragmentation, composition

1. Introduction

The formation of the terrestrial planets can be divided into several stages. Firstly, after the Sun's formation, the dust grains in solar nebula contacted directly and accreted into clumps of mm-to-meter in size. Planetesimals of 10 km in size have formed through the accretion of the clumps or directly from small grains.

Secondly, after the planetesimals formed in large number, runaway growth started. In runaway growth, the larger a body was, the faster it grew. This stage lasted between 10,000 and 100,000 years.

Thirdly, when the large bodies were massive enough to gravitationally perturb the residual planetesimals, a new phase, oligarchic growth began. This phase is characterized by the dominance of oligarchs, which continued to accreted planetesimals in their vicinities.

Lastly, when the embryos contained enough mass to interact with each other gravitational, merger stage followed. During this stage, the orbits of embryos became crossing and they gravitationally scattered one another strongly (Chambers 2013). The collisions and mergers between them allowed the embryos to grow to their present sizes.

Terrestrial planets are rocky planets which formed inside the frost line in solar system. Beyond the frost line, it is cold enough for hydrogen compounds to condense into solid ice grains, while inside it, there're many more solid grains available for accretion into planetesimals and planets. So the frost line separates terrestrial planets from jovian planets. For the terrestrial planets, they are composed largely of silicates and iron, which form their mantles and cores respectively.

The final structure of the planet system, the chemical compositions of the terrestrial planets and the timescale of their formation can be obtained by N-body simulations of the final stage of terrestrial planet formation. Previously, most studies dealt with collisions as

perfect mergers, which is obviously not the case in reality. A collision might turn out to be a partial accretion or erosion and involve fragmentation or hit-and-run.

According to the recent work of Leinhardt & Stewart (2012), collisions can be classified as merging, disruption, super-catastrophic disruption and hit-and-run. Through hydrodynamical simulations of planetary impacts, the authors identified the boundaries of different collision regimes, figured out the dependence of the mass and speed of the largest remnant on the impact energy, and fitted the mass and speed distributions of fragments. Applying this kind of detailed collision studies, Kokubo & Genda (2010) found that hit-and-run collisions are common, accounting for roughly half of collisions in the simulations. Comparing with the results of Chambers (2001) with merging only, Chambers (2013) found high collision rate, comparable formation timescale, mass reduction of final planets and so on. We are going to follow Chambers (2013) to perform N-body simulations of final stage of terrestrial planet formation.

Section 2 illuminates the numerical tool we use. Section 3 describes a realistic collision model we built based on the study of Leinhardt & Stewart (2012) in detail. Section 4 offers a method to track all the bodies' collision histories to calculate their composition fractions of silicate and iron. Section 5 summarizes the future work.

2. Tools

REBOUND is an N-body code designed for collisional dynamics, which is appropriate to our purpose. It can deal with classical N-body problems involving collision-less system and merger-only collisional system (Rein & Liu 2010).

We are going to expand its capability by adding code of dealing with different collision regimes. So a collision can result in different outcomes, probably involving fragmentation

and hit-and-run.

3. Collision modeling

3.1. Collision regimes

A specific collision scenario is clarified by these parameters: mass of target (M_t), mass of projectile (M_p), radius of target (R_t), radius of projectile (R_P), impact parameter (b) and impact speed (V_i). Specially, the impact parameter has a significant effect on the collision outcome because the energy of the projectile may not completely intersect the target when the impact is oblique. The above are the only needed parameters to identify its collision regime. It is assumed that the densities of two bodies are the same.

Figure 1 is a summary of major collision regimes defined by Leinhardt & Stewart (2012). The critical values of speed and impact parameter, V'_{esc}, $V_{erosion}$, $V_{supercat}$ and b_{crit}, are calculated following Leinhardt & Stewart (2012). According to the criteria in Figure 1, a collision can fall in a regime of merging, hit-and-run, disruption or super-catastrophic disruption.

At lower specific impact energies, the outcomes are merging, in which the target and the projectile merge into a single remnant with mass and momentum conserved.

Disruption regime refers to collisions in which the energy results in mass loss, the mass deference between the target and the largest remnant, between about 10% and 90% of the total mass. It's also defined as collisions that result in the largest remnant having a linear dependence on the specific impact energy.

The super-catastrophic regime is defined when the mass of the largest remnant is less than 10% of the total mass. And its mass follows a power law with impact energy rather

than the linear law.

In a hit-and-run collision, the projectile hits the target at an oblique angle but separates again, leaving the target almost intact.

3.2. The largest remnant

The largest remnant comes from the target after accretion or erosion resulting from the collision.

For merging, its mass is the total mass of target and projectile and its velocity is the velocity of center mass.

For disruption and super-catastrophic disruption, Leinhardt & Stewart (2012) gave following two explicit expressions of the mass of the largest remnant respectively, which were empirical fits of simulations.

$$M_{lr}/M_{tot} = -0.5(Q_R/Q'^{*}_{RD} - 1) + 0.5, \tag{1}$$

$$M_{lr}/M_{tot} = \frac{0.1}{1.8^{\eta}}(Q_R/Q'^{*}_{RD})^{\eta}, \tag{2}$$

where Q_R was the impact energy, Q'^{*}_{RD} was catastrophic disruption criteria-specific impact energy to disperse half the total mass and $\eta = 1.5$.

As to the largest remnant's velocity in the disruption and super-catastrophic disruption, the authors only provided two simple assumptions of its speed with respect to the center mass. Firstly, based on the assumptions, we derived the largest remnant's speed with respect to the center mass as summarized in Table 1, where gamma was the mass ratio of the projectile and the target. Secondly, we assumed that the direction of the velocity was the same as that of the target's velocity, so that the velocity of the largest remnant with respect to the center mass was obtained. Lastly, with the velocity of the center mass in

heliocentric frame, the velocity of the largest remnant in this frame was determined.

For hit-and-run, the mass and velocity of the largest remnant are approximately equal to the mass and velocity of target.

The location of the largest remnant in all the cases is simply assumed as the same as the target.

3.3. Fragments

Fragmentation can be involved in the regimes of disruption, super-catastrophic disruption and hit-and-run. The determinations of fragments' masses, velocities and locations are the same in all of them.

Based on their simulations, Leinhardt & Stewart (2012) came up with a differential relationship between the number and the radii of fragments,

$$n(R)dR = CR^{-(\beta+1)}dR, \tag{3}$$

where $n(R)$ was the number of objects with radii between R and $R + dR$, and C and β were constant parameters. So we deduced that the differential relationship between the mass and the radii was

$$dM = n(R)\frac{4}{3}\pi\rho R^3 dR, \tag{4}$$

and that a radius-binned mass, which meant the total mass of fragments with radii between R_{lower} and R_{upper}, was expressed as

$$M(R_{lower}, R_{upper}) = \frac{4}{3}\pi\rho C\frac{R_{upper}^{3-\beta} - R_{lower}^{3-\beta}}{3-\beta}. \tag{5}$$

Similarly, according to Leinhardt & Stewart (2012), the relationship between the mass

and the speeds of fragments with respect to the largest remnant is

$$log(\Delta v \frac{dm}{dv}) = A - Sv, \tag{6}$$

where dm is total mass of fragments with speeds between v and $v + dv$, m is in terms of the M_{tot}, v is in terms of V_{esc}, the escape velocity from the combined mass of the target and projectile, and A, S and Δv are constant parameters. We deduced that a velocity-binned mass, the mass of fragments with speeds between v_{lower} and v_{upper} with respect to the largest remnant, was

$$m(v_{lower}, v_{upper}) = \frac{10^{A-Sv_{lower}} - 10^{A-Sv_{upper}}}{S(ln10)\Delta v}. \tag{7}$$

So firstly, after we obtained every fragment's mass, its speed limits v_{lower} and v_{upper} were determined with this equation. Secondly, an averaged speed of the fragment was calculated to keep the integrated momentum not changed. Thirdly, we defined that all the velocities of fragments lied in the same plane consisting of the target, the projectile and the total momentum of the fragments in the frame of the largest remnant, so that by grouping fragments according to two different velocity directions to conserve total momentum, the velocities of fragments with respect to the largest remnant were determined. Lastly, given the velocity of the largest remnant in heliocentric frame, the fragments' velocities in heliocentric frame were obtained.

For the locations of fragments, we defined that they were on the same plane, which consisted the target, the projectile and the latter's velocity in the frame of the target. The largest remnant was at the position of target and the fragments were equal-spaced on a ring centered at the largest remnant with a proper radius to keep the bodies non-contacted. Then their position vectors in heliocentric frame were easily obtained.

4. Collision history tracking

To know the chemical compositions of planets at the end of the evolution, we have to keep record of the particles' composition fractions of silicate and iron. In other words, we have to know the collisions all the particles experienced.

The problem was settled with particle identifier (Figure 2). Each particle has its unique identifier ID0. However, it has a record of 3 more identifiers. ID1 and ID2 are the identifiers of its parents. This means from a collision between particle ID1 and particle ID2 was this particle ID0 produced. ID3 is to tell whether ID0 is a merger of this collision or a fragment from one of them, or a body existing in the initialization.

Figure 3 is an example to demonstrate how the collision history is constructed. The arrows point from each particle to its parents. In this case, particle 0 and particle 1 are the initial bodies with equal masses. After an energetic collision between 0 and 1, the second generation, particles with identifiers on the ring were produced. They are fragments of this collision. The third, fourth and fifth generations are the particles farther from the center. Many of them are mergers, such as 34, 35, 40, 42 and 43.

This method is helpful to calculate each particle's composition fractions of silicate and iron, given the initial compositions and the assumption that fragments of silicate are produced first followed by ones of iron if the total mass of fragments is larger than the total mass of silicate fractions of the target and projectiles.

5. Future work

We've adopted an equal-mass-fragment assumption for simplification. But a distributed-mass model is more realistic. We will try to include it into the collision model to make our model more capable. The next task is to perform the simulations in collision

model. The initialization of Chambers (2013) will be followed, meanly, 14 Mars-sized embryos, 140 Lunar-sized planetesimals, together with two giants, Jupiter and Saturn. At the same time, simulations with the same initialization but the realistic collision model will be going on. The collisions in the latter kind of simulations will only result in mergers.

A lot of study can be inspired by the simulation results. We currently focus on the structure of the final planet system including the final number and positions of planets, the timescale of terrestrial planet formation, the compositions of the planets and so on. We'll see what difference the realistic collision model can make by comparing the two groups of simulation results.

We are grateful to ISIMA 2014 for providing a precious opportunity for us to meet and to work together efficiently.

REFERENCES

Chambers, J. E., 2001, Icarus, 152, 205

Chambers, J. E., 2013, Icarus, 233, 83

Kokubo, E. & Genda, H., 2010, ApJ, 714, L21

Leinhardt, Z. M. & Stewart, S. T., 2012, ApJ, 749, 79

Rein, H. & Liu, S.-F., 2012, å, 537, A128

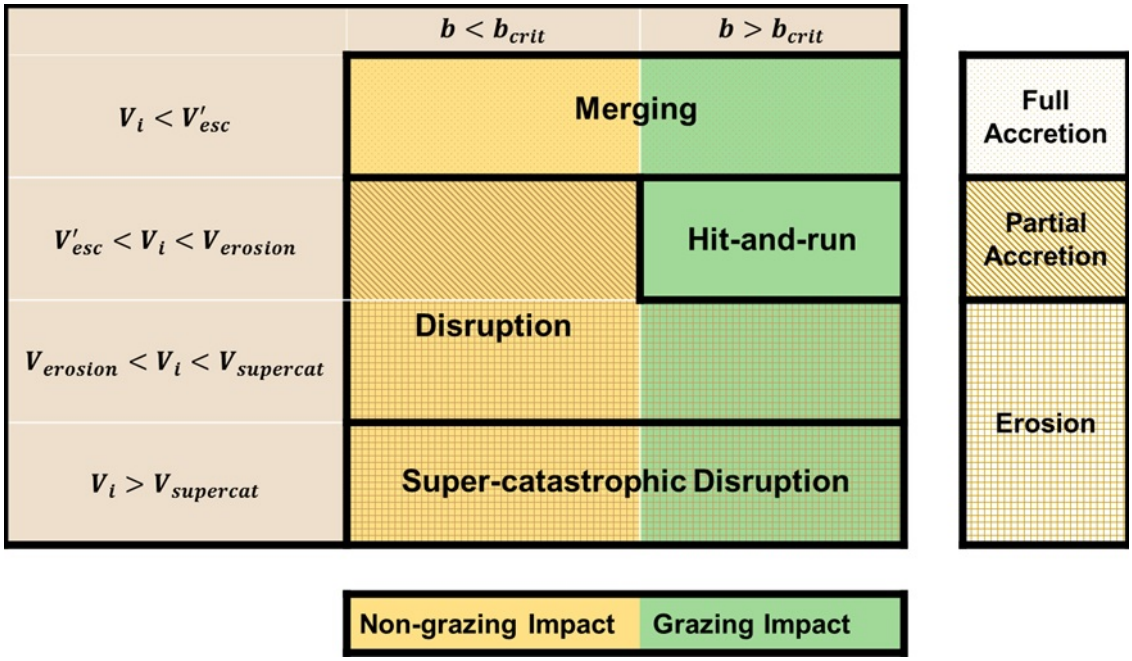

1.jpg

Fig. 1.— Summary of major collision regimes defined by Leinhardt & Stewart (2012).

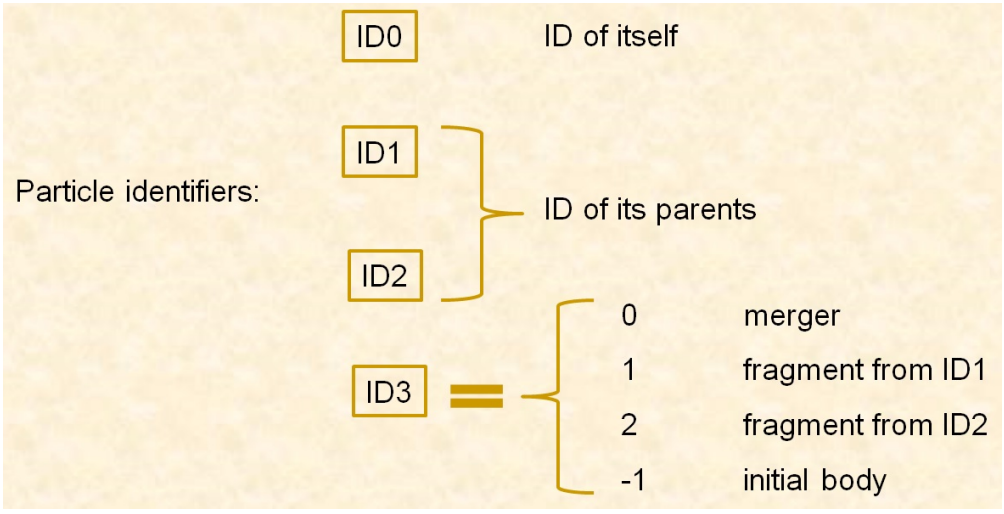

2.jpg

Fig. 2.— Particle identifiers.

3.jpg

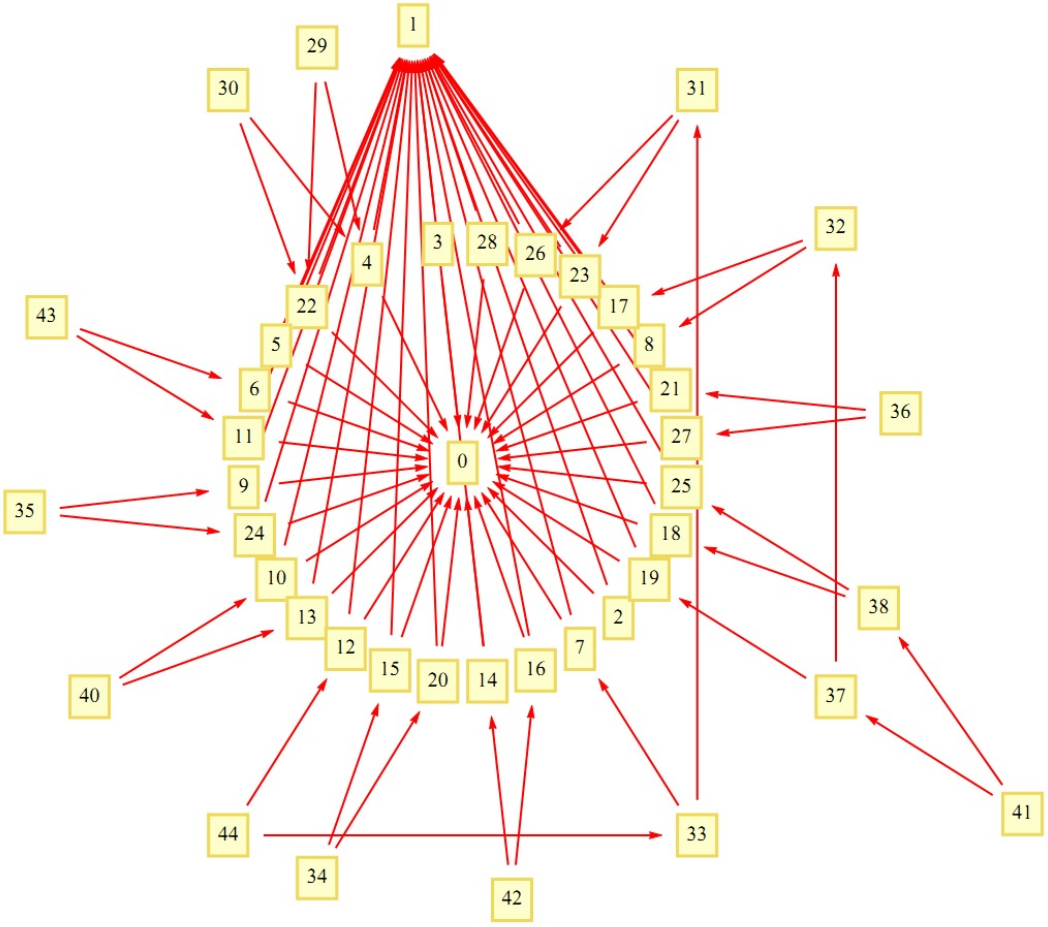

Fig. 3.— An example to demonstrate how the collision history is constructed. The arrows point from each particle to its parents.

Table 1. Speed of the largest remnant with respect to the center mass

	$0 \leq b \leq 0.7$	$b > 0.7$
$\frac{M_{lr}}{M_t} \leq 1$	$\frac{b}{0.7} V_t$	V_t
$1 < \frac{M_{lr}}{M_t} \leq 1 + \gamma$	$\frac{bV_t}{0.7\gamma}[-\frac{M_{lr}}{M_t} + (\gamma + 1)]$	$\frac{V_t}{\gamma}[-\frac{M_{lr}}{M_t} + (\gamma + 1)]$